P5F.2 COMPARISON OF OBJECTIVE ANALYSIS SCHEMES FOR THE WSR-88D RADAR DATA

Jian Zhang[1], Ken Howard[2], Wenwu Xia[1], J. J. Gourley[1]
[1]Cooperative Institute for Mesoscale Meteorological Studies, Norman, OK
[2]NOAA/National Severe Storms Laboratory, Norman, OK

1. INTRODUCTION

The advent of Internet-2 and effective compression techniques facilitates the transmission of the full base level radar data from NEXRAD (NEXt generation RADar, http://www.roc.noaa.gov/) network economically and in real-time as demonstrated by the CRAFT (The Collaborative Radar Acquisition Field Test, Droegemeier et al. 2000) network. The result is the ability to integrate the full resolution base level data from multiple radars into a three dimensional framework at high-resolution time and space scales.

The integration and display of multiple radar data is very useful for the National Weather Service (NWS) and for aviation communities. Many NWS county warning areas (CWA) span multiple radar umbrellas. The ARTCCs (Air Route Traffic Control Centers) of FAA (Federal Aviation Administration) cover even larger areas than the CWAs. Further, weather systems often extend over multiple radar coverages. The FAA and NWS operations require bringing multiple radar data onto a common grid (Zhang et al. 2001).

Due to the spherical coordinates of WSR-88D (Weather Surveillance Radar -- 1988 Doppler) radar data sampling system, the data resolution is extremely non-uniform in space. This non-uniformity, together with largely variable spatial scales of weather systems, poses a significant challenge to objective analysis of radar data. In this paper we will present various objective analysis methods applied to WSR-88D data for different weather regimes. These include comparisons of radar bin volume mapping, nearest neighbor, and linear interpolation for gridding and nearest neighbor, maximum value, and distance weighted mean techniques for mosaicking.

The gridding schemes mentioned previously will be presented in section 2 and mosaicking schemes in section 3 with a summary in section 4.

2. GRIDDING SCHEMES

Four interpolation schemes were tested for remapping radar data from polar coordinates onto Cartesian coordinates. The first scheme, radar bin volume mapping (RBVM), simply fills in grid cells within a given radar bin volume with the value observed at the co-located bin. All grid cells that are not covered by any radar bin volume are flagged as missing. The second scheme, nearest neighbor mapping (NNM), is where each grid cell gets a value from the nearest data bin (based on the distance between center of the grid cell to the center of the radar data bin). The third scheme is a nearest neighbor scheme on range-azimuth planes combined with a linear interpolation in elevational direction. For small elevation angles (<20°), the vertical direction is close to the elevational direction. Thus this scheme will be referred as vertical interpolation (VI) scheme. The fourth scheme uses the VI plus a horizontal interpolation to fill in the gaps between higher tilts.

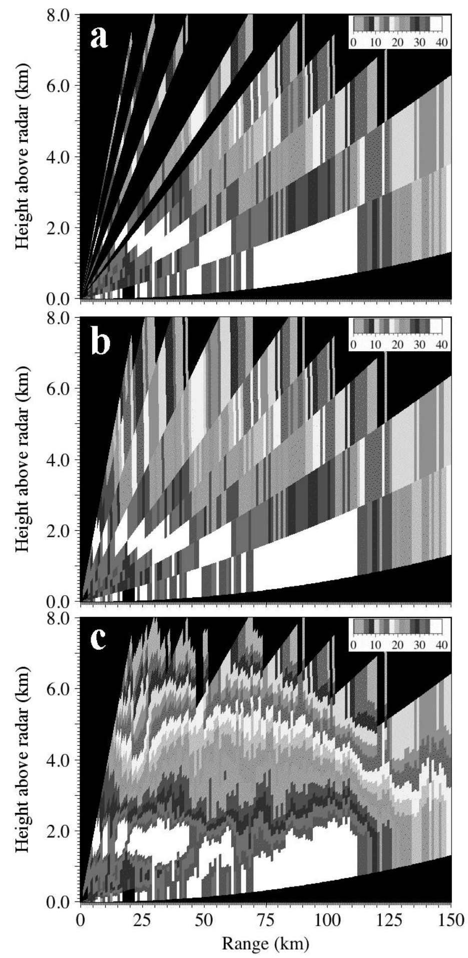

Fig. 1 Range height indicator (RHI) plots of reflectivity field along 0° azimuth from KIWA at 0859Z on 19 February 1998 using a bin volume mapping (a), a nearest neighbor (b), and a vertical linear interpolation (c) schemes.

Corresponding author address: Jian Zhang, NSSL, 1313 Halley Circle, Norman, OK 73069.
Email: jian.zhang@noaa.gov

The NNM scheme (Fig.1a) shows the beam geometry with the 4/3 effective earth's radius model (Doviak and Zrnic, 1984) and the resulting gaps between the higher tilts. The gaps are more pronounced for VCP (volume scan pattern) 21 than for VCP 11. Nearest neighbor approach filled in the gaps, yet discontinuities exist between tilts (see clearly defined beam boundaries between tilts in Fig.1b). The discontinuities were caused by the reflectivity differences between two neighbor bins on adjacent tilts. The difference becomes large when the centers of the two bins are further away (at far ranges) because the reflectivity value in any given radar bin is largely dominated by targets near the center of the bin. By performing a linear interpolation in the elevational direction, the discontinuities are successfully removed (Fig.1c). But when a stratiform cloud/precipitation system with very strong vertical gradient (e.g., a bright-band layer) exists, the VI scheme failed to recover horizontally extended layers in the data void regions (e.g., at height of 1.9km, and at ranges of 8, 13, and 19km, Fig.1c). This resulted in ring-shaped artifacts (at those above-mentioned ranges) on horizontal cross sections in the interpolated fields (Fig.2a). It was found

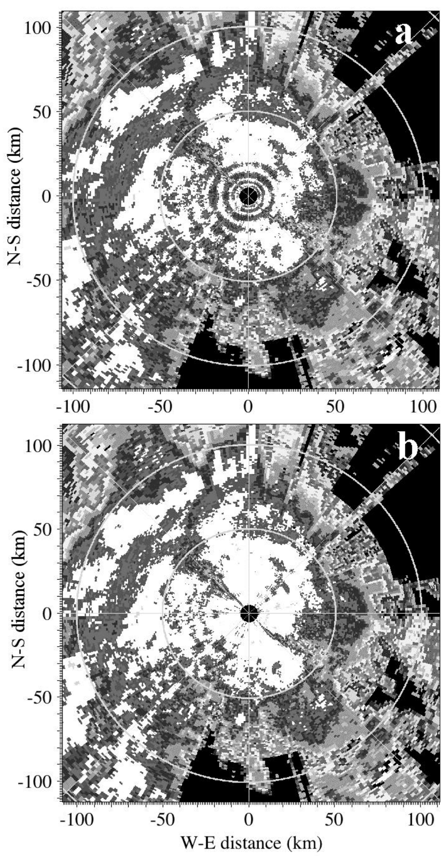

Fig. 2 Horizontal cross sections at 1.9km above radar level from the 3D reflectivity analyses of KIWA data by vertical linear interpolation (VI) (a) and the VI plus an additional horizontal interpolation (b).

that a horizontal interpolation in the data voids, in addition to the VI scheme, can remove the ring-shaped artifacts and recover the bright-band feature (Fig.2b). However, the horizontal interpolation should be applied only for stratiform echoes and with a horizontal scale constraint. For upright convective storms with strong horizontal gradients (Fig.3a), the VI scheme alone produces very reasonable analysis (Fig.3b). Additional horizontal interpolation can smooth the strong horizontal gradients or even reduce the intensities of the storms if the analysis grid resolution is coarse and storms are close to the radar.

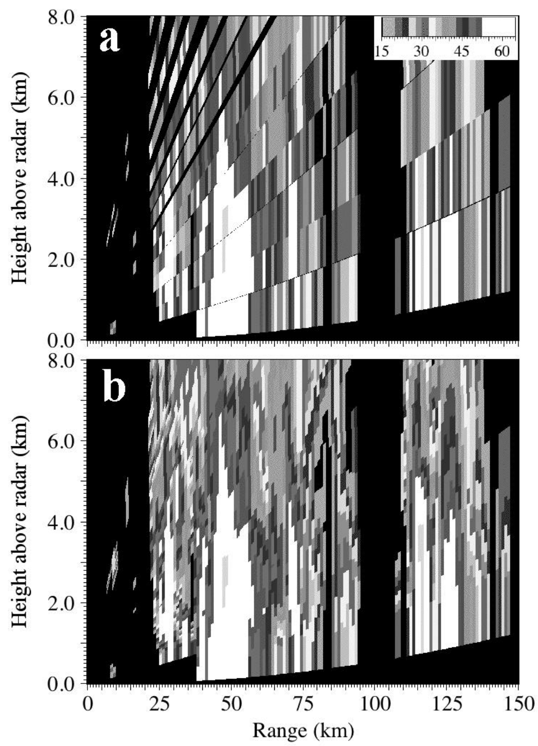

Fig.3 Range height indicator (RHI) plots of reflectivity field along 263° azimuth from KIWX at 2036Z on 25 June 2002 using a bin volume mapping (a) and a vertical linear interpolation (b) schemes.

3. MOSAIC SCHEMES

After reflectivity fields from individual radars are remapped onto the Cartesian grid, they are combined to produce a unified 3D reflectivity grid. There are many regions, especially at upper levels of the atmosphere, in the United States that are covered by multiple radar umbrellas (Maddox et al., 2002). For grid cells not covered by any radar observation volume (e.g., below the lowest and above the highest radar tilts), missing values are assigned. For grid cells with only one radar coverage, the analysis value from that radar is assigned. For grid cells with multiple radar coverage, the following three schemes are tested.

The first scheme is the nearest neighbor scheme where the analysis value from a radar that is closest to the grid cell is assigned. The nearest neighbor scheme does not impose any smoothing when combining multiple radar fields. However, discontinuities sometimes appear at the equidistant lines between radars in the mosaicked field. Figs. 4a and 4b show composite reflectivity fields from two nearby radars (KIWX at Ft. Wayne, Indiana and KLOT at Chicago, Illinois) on a common grid, and their difference is shown in Fig.4c. The KIWX composite reflectivity values are significantly higher than the KLOT and dominated the majority of the domain (Fig.4c). The mean difference (KIWX-KLOT) between the two radar's composite reflectivity observations at the equidistant grid cells is +7.67dBZ. Studies have shown that calibration differences among WSR-88Ds often exist and sometimes the differences can be significant (Gourley et al. 2003). The calibration differences result in discontinuities in the nearest neighbor mosaic along the equidistant lines (Fig.4d). Therefore the nearest neighbor scheme is not recommended for 3D mosaic especially when the analysis grid will be used in numerical models.

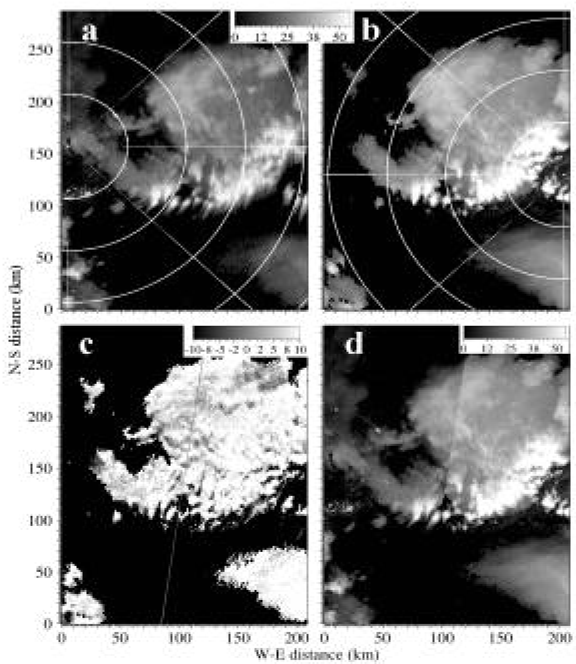

Fig.4 Composite reflectivity fields from KLOT (panel a) and KIWX (panel b) radars valid at 2036Z on 25 June 2002. Panel c shows the difference between the two composite reflectivity fields (panel b - panel a). The difference field shows positive values in most of the storm regions. The gray line in panel c indicates the equidistance line between the two radars. Panel d shows the mosaic of the two fields in panels a and b using a nearest neighbor scheme. A discontinuity at the equidistance line between KIWX and KLOT is apparent.

The second scheme is to take the maximum among the analysis values from multiple radars. This method does not impose any smoothing, and it will assure that the intensity of the strongest storms will be retained in the analysis. However, it can also produce discontinuities in the analysis fields. For cases where a bright-band layer exists, the fine, high intensity layer observed by a close-by radar may be smeared by degraded observations from a far-away radar due to beam spreading.

Given the fact that the calibration differences may exist at any given time, a weighted mean scheme is preferred to avoid discontinuities in the mosaic fields. Two weighting functions, both based on distances between a given grid cell and the multiple radars covering the grid cell, are tested. The first is a Cressman scheme with 300km radius of influence (Fig.5) and the second is an exponential function with 50km distance scale (Fig.5). The Cressman weighting function resulted in reductions of high storm intensities observed by radars close to the storms (compare Figs.6a and 4b). This results from the Cressman weighting function being relatively too flat and provides too much weight to radar observations at far ranges (Fig.5). The exponential weighting function, on the other hand, provides a smooth mosaic field while retaining the magnitude of the observations from the close radar (compare Figs.6b and 4b).

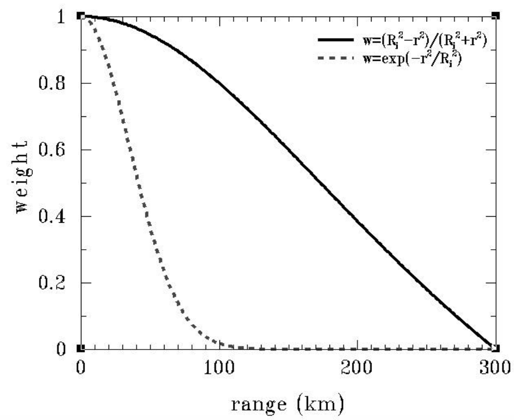

Fig.5 The Cressman and the exponential weighting functions used to generate mosaic fields shown in Fig. 6.

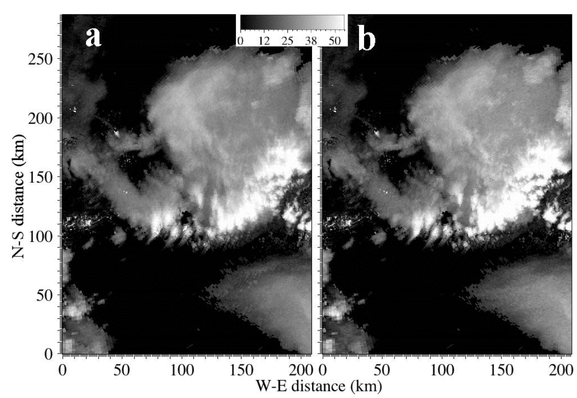

Fig.6 Mosaic composite reflectivity fields of the KIWX and KLOT observations using a Cressman weighting function with 300km radius of influence (panel a) and a exponential weighting function with a length scale of 50km (panel b).

4. SUMMARY

Four interpolation schemes and three mosaic schemes are presented in this paper. These techniques are used to convert multiple radar reflectivity data from their native (polar) grid onto a mosaicked 3D Cartesian grid. After experimenting with different weather regimes including spring/summer time convective storms and wintertime stratiform precipitation systems, it was found that the vertical interpolation scheme with nearest neighbor on the range-azimuth plane provides the most physically realistic mosaic for the convective storms. For stratiform precipitation, an additional horizontal interpolation scheme is required in reconstructing the horizontally extended layers in the data voids (e.g., between upper tilts in VCP 21). When combining multiple radar analysis fields onto a single 3D grid, a distance weighted mean scheme is preferred to produce a continuous field. The shape of the weighting functions is important for retaining the intensities of storms.

5. ACKNOWLEGEMENTS

Funding for this research was provided under the FAA NAPDT (NEXRAD Algorithms Product Development Team) MOU.

6. REFERENCE

Doviak, R.J., and D.S. Zrnic, 1984: Doppler Radar and Weather Observations, Academic Press, Inc., Orlando, 458 pp.

Droegemeier, K.K., K. Kelleher, T.D. Crum, J. Levit, S.A. DelGreco, L. Miller, C. Sinclair, M. Benner, S.W. Fulker, and H. Edmon: Project CRAFT: A test bed for demonstrating the real time acquisition and archival of WSR-88D Level II Data, *Preprints*, 18th IIPS, Orlando, FL, Amer. Meteor. Soc., 136-139.

Gourley, J.J., B. Kaney, and R.A. Maddox, 2003: Evaluating the calibrations of radars: a software approach. *Preprints, The 31st International Radar Conference,* Aug 6-12, Seattle, Washington.

Maddox, R.A., J. Zhang, J.J. Gourley, and K. Howard, 2002: Weather radar coverage over the contiguous United States. *WAF*, 17, 927-934.

Zhang, J.,J. J. Gourley, K. Howard, B. Maddox, 2001: Three-dimensional gridding and mosaic of reflectivities from multiple WSR-88D radars. *Preprints, The 30th International Radar Conference,* July 19-24, Munich, Germany, 719-721.